[Research Paper] 대한금속 · 재료학회지 (*Korean J. Met. Mater.*), Vol. 62, No. 1 (2024) pp.57-64
DOI: 10.3365/KJMM.2024.62.1.57

Thermomechanical Behavior and Microstructure Properties of Carbon Fiber Reinforced Polymer at Elevated Temperatures

Okmin Park[1,†], Seulgi Han[2,†], Sanghyun Park[1], Jamil Ur Rahman[3], Sang-il Kim[1,*], and Sungmo Choi[2,*]

[1]*Department of Materials Science and Engineering, University of Seoul, Seoul 02504, Republic of Korea*
[2]*Department of Architectural Engineering, University of Seoul, Seoul 02504, Republic of Korea*
[3]*Leibniz Institute for Solid State and Materials Research, Dresden 01069, Germany*

Abstract: Carbon fiber reinforced polymer (CFRP) has been extensively used in civil engineering for applications such as reinforcing and retrofitting various architectural materials. Therefore, understanding the degradation of CFRP under high temperatures is important. This study aims to investigate the thermo-mechanical and microstructural properties of CFRP plates at elevated temperatures up to 350 °C. The plate-type CFRP composites were subjected to temperatures of 50, 100, 150, 200, 250, 300, and 350 °C, and then compared with pristine CFRP samples. X-ray diffraction analysis was conducted to examine the crystal structures of the carbon fibers and epoxy resin matrices in the CFRP. At temperatures higher than 150 °C, the FWHM increased due to the degradation and softening of the resin matrix. Delamination and debonding between the matrix and fibers were observed in samples exposed to temperatures above 200 °C. The maximum tensile strength of the CFRP plates exposed at 350 °C significantly decreased to 0.605 GPa, a reduction of approximately 40% compared to the pristine sample. On the other hand, Young's modulus remained relatively unchanged across the different temperatures. This suggests that the polymer matrix degradation plays a crucial role in the mechanical properties of CFRP, as the matrix layers contribute significantly to the distribution of forces.

(Received 21 September, 2023; Accepted 25 October, 2023)

Keywords: carbon fiber reinforced polymer, thermal degradation, tensile stress

1. INTRODUCTION

Research on polymer composites based on carbon-related materials is actively being conducted due to their superior properties [1,2]. Carbon fiber-reinforced polymer (CFRP). provides numerous advantages, including high tensile strength/weight ratios, tensile modulus/weight ratios, low coefficient of thermal expansion, high fatigue strengths, and thermal conductivity [3,4]. Since the development of carbon fiber in the 1960s, CFRP has found wide-ranging applications in fields including civil engineering, shipbuilding, aircraft manufacturing, and aerospace [5-10]. In civil engineering, CFRP has proven particularly useful, with studies focusing on beams made of reinforced concrete (RC) or wood as representative examples of CFRP-reinforced structures [7,11–13]. Additionally, CFRP cables are extensively used in civil structures like suspension bridges and large structure roofs [14–19].

In the field of structural beam engineering, Täljsten and Elfgren [11] proposed various methods and tests for applying CFRP fabrics and tapes to concrete beams in 2000. They employed three different reinforcement methods using CFRP: two hand lay-up systems, one vacuum injection system, and one pre-preg system. Their test results demonstrated a maximum strengthening effect of approximately 300%. CFRP can also be used to reinforce wood beams, as highlighted by Borri et al. [13], who found that CFRP sheet-reinforced wood beams exhibited an increase in flexural capacity of up to 60.3% compared to unreinforced beams. They also noted that the use of CFRP

†These authors contributed equally to this work.
- 박옥민:석사과정, 한슬기:석사과정, 박상현:학부생, Jamil Ur Rahman: 선임연구원, 김상일: 교수, 최성모: 교수
**Corresponding Author:* Sang-il Kim
[Tel: +82-2-6490-2414, E-mail: sang1.kim@uos.ac.kr]
**Corresponding Author:* Sungmo Choi
[Tel: +82-2-6490-2796, E-mail: smc@uos.ac.kr]

bars for reinforcement resulted in smaller increases in flexural capacity compared to CFRP sheet reinforcement.

In bridge engineering, researchers, including Meier and others, are actively exploring the replacement of steel wires with CFRP cables [14, 15, 19]. Moreover, the Swiss Federal Laboratory for Materials Testing and Research (Empa) has been continuously developing prestressed CFRP for strengthening RC structures [20]. Their studies have focused on the flexural and shear strengthening of RC structures using prestressed CFRP. According to a review paper written by Pawlak et al. in 2022 [21], CFRP is currently employed as structural reinforcements in numerous fields as well as building engineering. In addition, recent studies have mainly been performed to investigate the environmental factors of composite structures, such as their recycling and evaluation for pollution compared to other building materials [22, 23].

To use CFRP as a reinforcement material, it is necessary to be mindful of certain weaknesses. The primary weaknesses of CFRP include degradation at elevated temperatures, high cost, low ductility, and low shear strength [21]. The degradation of CFRP due to the low thermal decomposition temperature (approximately 250–350 ºC) of the polymer matrix at elevated temperatures has drawn significant attention [22-24].

While carbon fibers have an extremely high ignition temperature (approximately 2000 ºC) compared to the polymer matrix, the degradation properties of CFRP are mainly determined by the glass transition temperature (T_g) and decomposition temperature (T_d) of the polymer matrix [25]. When exposed to temperatures above T_g, the polymer matrix softens and becomes rubbery, leading to degraded mechanical properties due to reduced bonding strength between the fibers. Exposure to temperatures above T_d causes the matrix to decompose, releasing toxic fumes and undergoing phase transformation, resulting in a significant reduction in the mechanical performance of CFRP materials [26–28].

Therefore, in recent years, numerous studies have been conducted on the heat deterioration of CFRP under elevated temperatures [29–34]. Cao et al. [29] prepared CFRP and hybrid FRP composites and investigated their mechanical properties after exposure to temperatures ranging from 16 to 200 ºC. Their results showed a significant decrease in the tensile strengths of CFRP composites with increasing temperature. Lee et al. [32] studied the hardness and microstructure of various types of CFRP from room temperature to 350 ºC. They reported a hardness decrease of up to 30% as the temperature increased. Additionally, they demonstrated the gradual deterioration of the polymer matrix with increasing temperature, through microstructure observations.

On the other hand, Park et al. [34] investigated the mechanical properties of recycled CFRP chips consisting of a phenolic resin matrix at different elevated temperatures ranging from 200–600 ºC. They confirmed an enhancement in mechanical properties at certain elevated temperatures, suggesting that appropriate temperature can increase the interfacial adhesion between the fibers and the matrix. In this study, plate-shaped CFRP specimens with an epoxy resin matrix were prepared to observe the various behaviors of CFRP at T_g and T_d. These specimens were exposed to different temperatures ranging from 50 to 350 ºC for 30 minutes. The microstructures of CFRP were observed after exposure to the different temperatures, and the tensile strength and thermal transport properties of each sample were measured and analyzed.

2. EXPERIMENTAL

Plate-type CFRP composites (Toray, Tokyo, Japan) were prepared using the pultrusion process, with a matrix of epoxy resin. The pristine plate-type CFRP, denoted C000, had dimensions of 50 mm width, 50 mm length, and 1 mm thickness. To investigate the effects of different temperatures, the C000 samples were exposed at temperatures ranging from 50 – 350 ºC at intervals of 50 ºC for 30 min. The samples were designated C050, C100, C150, C200, C250, C300, and C350, corresponding to the exposure temperatures. The process involved placing the samples in a muffle furnace in air for 30 min., followed by slow cooling in the furnace. The crystalline phases of the samples were identified using X-ray diffraction (XRD) with a voltage of 40 kV and a current of 40 mA. The XRD analysis was conducted in the 2θ range of 10º–60º with a scan speed of 3º/min, using Cu $K_{\alpha 1}$ radiation. Field emission scanning electron microscopy (FESEM) was performed to observe the surface

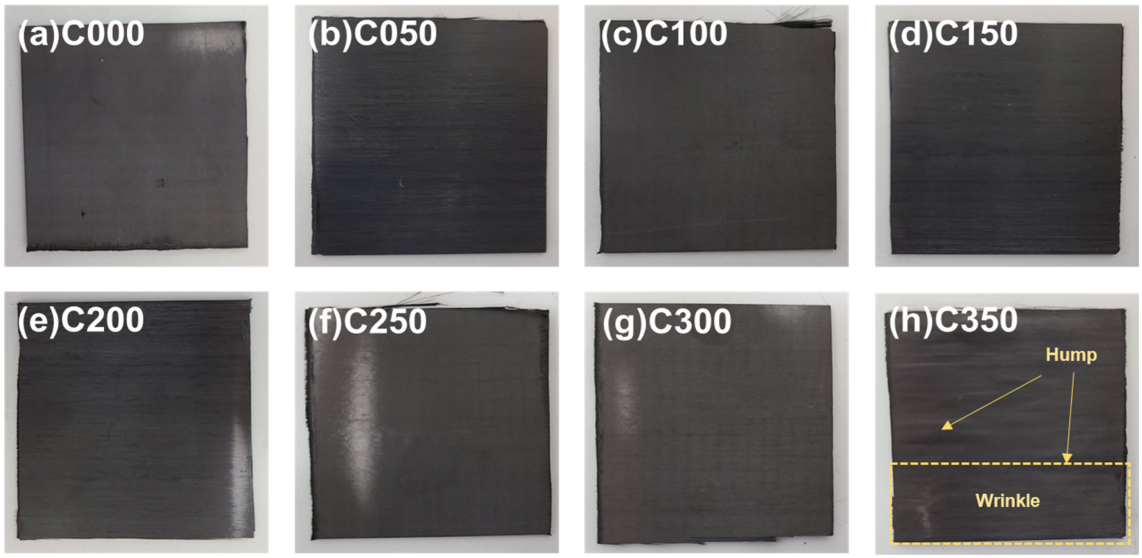

Fig. 1. Photographs of CFRP plates: (a) C000, (b) C050, (c) C100, (d) C150, (e) C200, (f) C250, (g) C300, and (h) C350 samples

microstructures of the samples. The sample surfaces were coated with Pt for FESEM observation. The thermal conductivity (κ) of the samples was calculated using the relationship $\kappa = \alpha \cdot \rho \cdot C_p$, where α represents the thermal diffusivity, ρ denotes the density, and Cp indicates the specific heat capacity of the sample. The α and Cp values were obtained using laser flash analysis (LFA) conducted at temperatures ranging from 27 to 150 °C, and the ρ value was estimated based on the mass/volume of the samples. Estimated ρ values for samples along the firing temperature 0–350 °C were 1.66, 1.64, 1.67, 1.66, 1.64, 1.61, 1.60, 1.55 g/cm^3, respectively. The mechanical properties of the samples were measured using a universal testing machine.

3. RESULTS AND DISCUSSION

Photographs of each sample, C000–C350, are shown in Figure 1.

Upon visual inspection, no significant differences were observed from C000 to C300. However, the C350 sample (Figure 1(h)) exhibited distinct features, including a wavy pattern, humps, and dents on the surface. These damages in the C350 sample were attributed to interlaminar failure caused by the high interlaminar stresses developed between the layers of the fibers [32, 35, 36]. Additionally, the high heat treatment promoted the diffusion of air trapped within the polymer matrix, from the inside to the outside [28]. Consequently, these phenomena resulted in surface expansion and the formation of numerous pores.

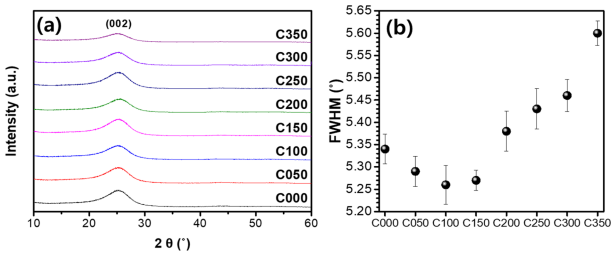

Fig. 2. (a) XRD patterns and (b) calculated FWHM of C000, C050, C100, C150, C200, C250, C300, and C350 samples

Figures 2(a) and 2(b) present the XRD patterns and full width at half maximum (FWHM) of the samples, respectively. The XRD patterns exhibited a typical form with the main peak at 25.5°, similar to other CFRP composites [28, 37]. An amorphous halo centered at approximately 18° was observed due to the epoxy resin matrix [38], and its amorphous tendencies became more pronounced at 200 °C or higher, as confirmed by the calculation of FWHM. FWHM is a reliable indicator of the amorphous transformation behavior of the resin matrix, as it is inversely proportional to the grain size [39, 40]. Additionally, the FWHM scale reflects the short-range order of amorphous materials [41]. Hence, an increase in FWHM indicates a reduction in the short-range molecular order within the amorphous structure, and this

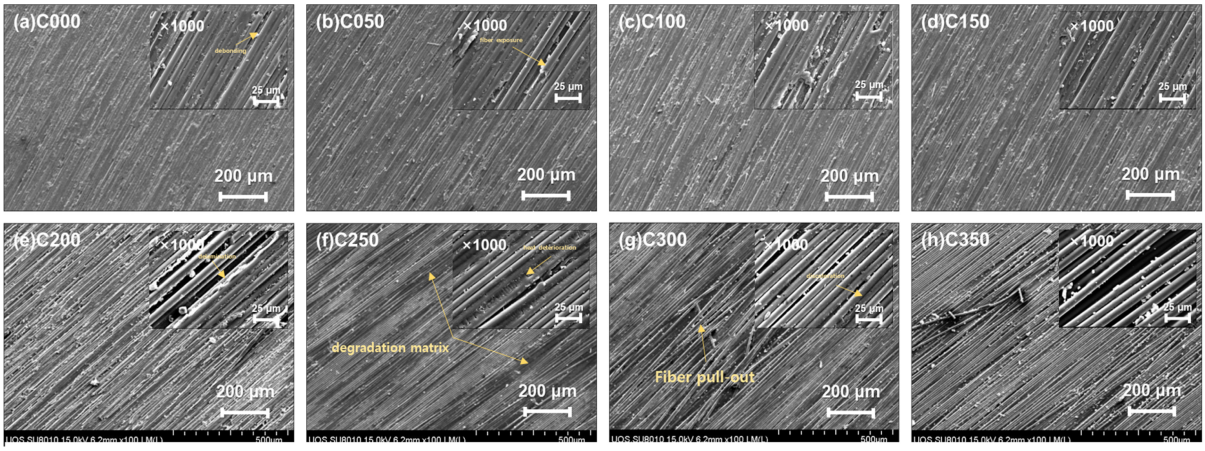

Fig. 3. FE-SEM images of CFRP plates: (a) C000, (b) C050, (c) C100, (d) C150, (e) C200, (f) C250, (g) C300, and (h) C350 samples (Inset in each figure is a highly magnified version of the image (×1000))

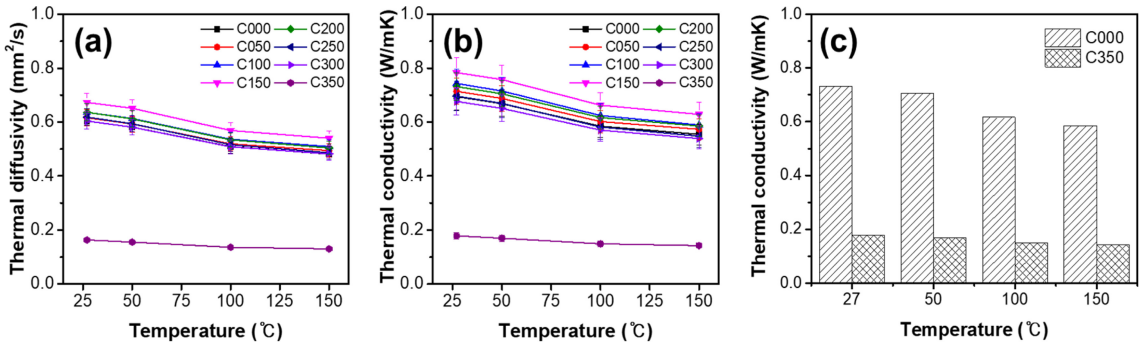

Fig. 4. Thermal transport properties of CFRP plates: (a) α, (b) κ, and (c) comparison of the κ between C000 and C350

phenomenon indirectly shows an increase in the amorphous-state because it is inversely proportional to crystallinity.

The decrease in FWHM values in the C050, C100, and C150 samples can be attributed to a common characteristic of thermo-setting polymers, which undergo a hardening process at specific temperatures. However, for the C200, C250, C300, and C350 samples, the FWHM values gradually increased with the temperature, surpassing those of the C000 sample. These results clearly demonstrate that exposure to temperatures above 200 ºC leads to degradation and softening of the resin matrix.

Figure 3 depicts the microstructure of the CFRP composites, with high-magnification images provided as insets. The microstructures of the C000 to C150 samples remained unchanged despite the variations in temperature. These samples exhibited minimal physical scratches and defects, such as fiber breakage or micro-cracks. However, the C200 sample showed signs of degradation due to the heat treatment, with several instances of delamination observed in its matrix. These findings aligned with the XRD results, where the C050, C100, and C150 samples exhibited lower FWHM values compared to the C000 sample, while the C200, C250, C300, and C350 samples showed higher FWHM values. As the temperature increased, the degradation of the epoxy matrix in the CFRP, including heat deterioration, fiber pull-out, and delamination, became more pronounced. Eventually, the resin matrix in the C350 sample was completely decomposed, exceeding its T_d (decomposition temperature).

Figures 4(a) and 4(b) present the measured and calculated thermal transport properties. At 300 K, the κ values for C000, C050, C100, C150, C200, C250, and C300 were 0.70, 0.71, 0.74, 0.78, 0.73, 0.70, and 0.68 W/mK, respectively. The trends in the thermal transport properties of the samples closely matched the FWHM trends (Figure 2(b)), indicating the crystallinity plays a significant role in the thermal

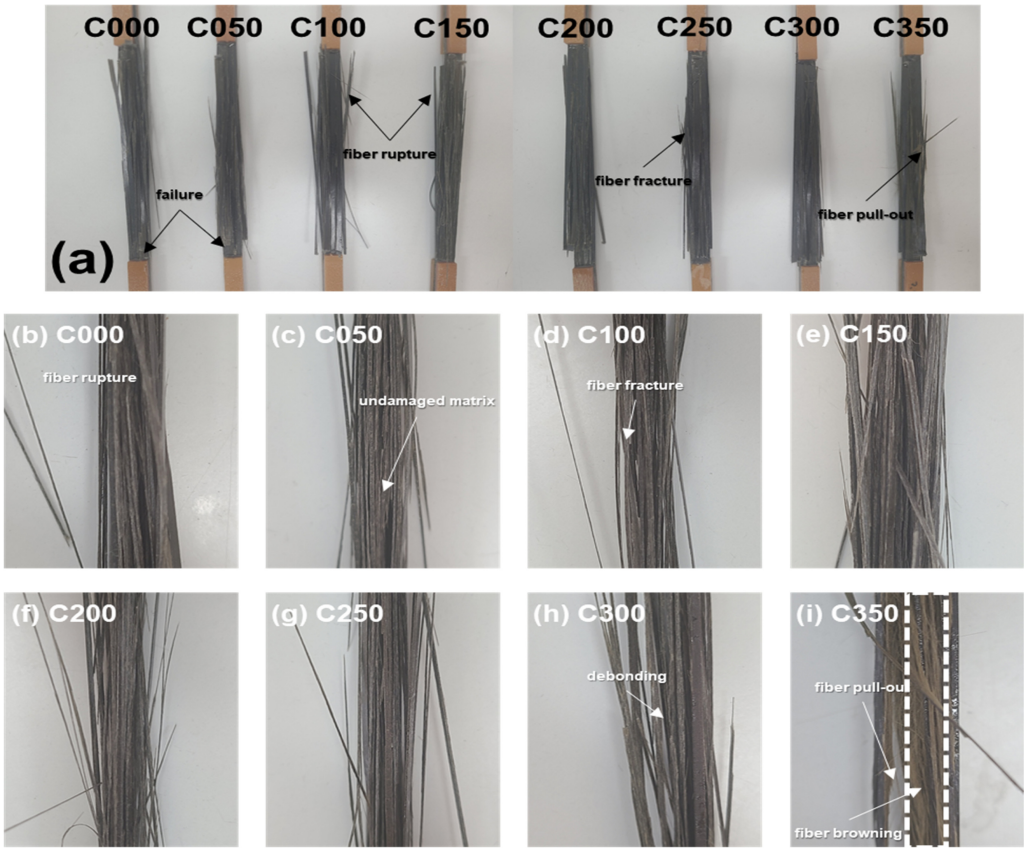

Fig. 5. (a) Top-view and (b)–(i) cross-sectional failure modes of the specimens

Table 1. Values of maximum force, σ_{max}, ε_{max}, and E for the samples.

Sample	Maximum force (kN)	σ_{max} (GPa)	ε_{max} (%)	E (GPa)
C000	125.2 ±4.0	1.04 ±0.03	0.019 ±0.001	53.2 ±0.8
C050	133.2 ±9.6	1.10 ±0.09	0.020 ±0.001	55.4 ±1.1
C100	138.0 ±12	1.15 ±0.06	0.019 ±0.001	55.5 ±1.5
C150	145.2 ±16	1.21 ±0.14	0.020 ±0.001	54.7 ±0.8
C200	130.4 ±7.6	1.09 ±0.07	0.019 ±0.001	54.6 ±0.4
C250	127.5 ±11	1.06 ±0.1	0.018 ±0.002	55.2 ±0.8
C300	119.8 ±11	1.00 ±0.09	0.018 ±0.001	55.2 ±0.8
C350	72.5 ±7.0	0.605 ±0.06	0.011 ±0.001	52.0 ±0.1

transport mechanism of the FRP composites, primarily through phonon scattering [42–44]. The significant reduction in thermal transport properties observed in the C350 sample (κ = 0.18 W/mK) compared to the other samples (Figure 4(c)) can be attributed to the increased phonon scattering resulting from decreased crystallinity. The delamination of the matrix layer generates numerous pores and weakens the bonding between the fibers. Consequently, the κ value of the C350 sample experiences a significant decrease, of 3.9 times compared to the C000 sample.

The failure modes of the samples with different temperatures are depicted in Figure 5, and the results of the tensile tests are listed in Table 1.

Similar failure modes were observed from C000 to C300, where failures occurred at the end part of the samples during the tensile test, except for C350. In the case of C000 to C150,

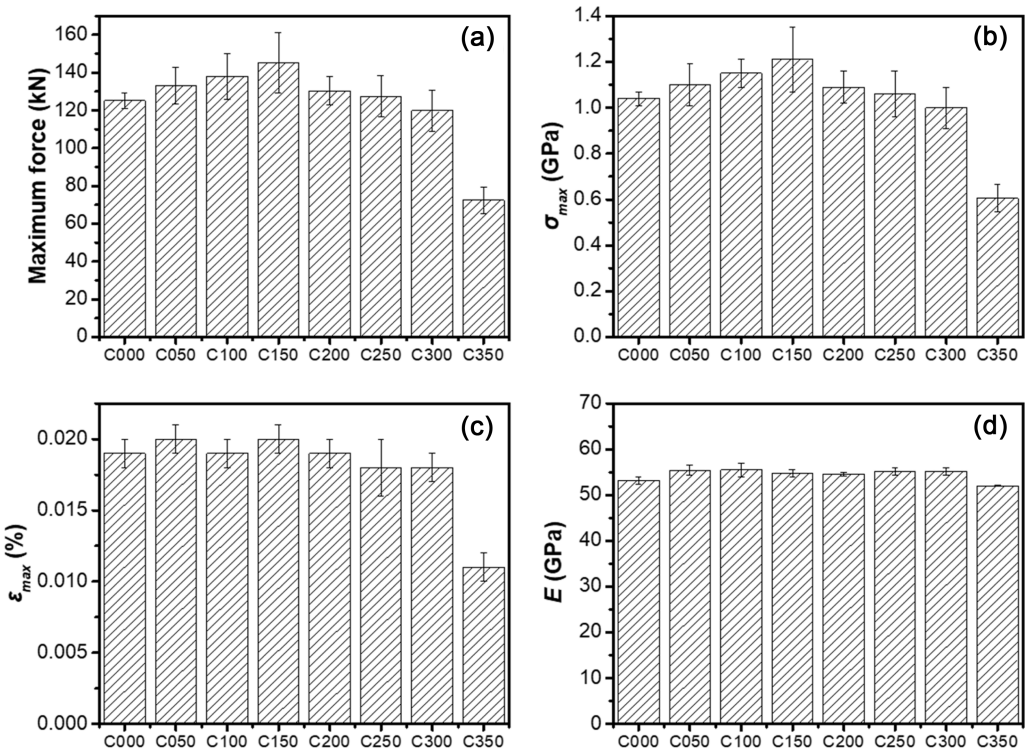

Fig. 6. Mechanical properties of the samples: (a) maximum force, (b) σ_{max}, (c) ε_{max}, and (d) E

undamaged matrix layers were present, contributing to an even distribution of applied stress along with the fibers.

Additionally, properly heat-treating thermosetting polymers is known to enhance the interfacial adhesion between the fiber and polymer matrix [34]. Therefore, the mechanical properties of C050, C100, and C150 samples were generally improved compared to those of the C000 sample, as shown in Figure 6.

The maximum tensile strength (σ_{max}) values for C000, C050, C100, and C150 were 1.04 to 1.10, 1.15, and 1.21 GPa, respectively, representing an enhancement of up to 16%. The maximum tensile forces also increased to 145 kN compared to the pristine CFRP, which had a maximum tensile force of 125.2 kN. In contrast, σ_{max} of the C200–C300 samples gradually decreased to 1.09–1.00 GPa (Figures 6(a) and 6(b)) due to deterioration of adhesion between the matrix and fiber, as shown in Figures 5(e) to 5(g) which show delamination and debonding.

The C350 specimen, exposed to a temperature exceeding T_d (Figure 5(h)), exhibited fiber browning and fiber pull-out. The discoloration of C350 is attributed to the infiltration of decomposed epoxy resin into the fibers and the oxidation of fibers [44, 45]. Wang et al. [46] investigated the change in the failure mode of CFRP composites over a temperature range of 22–706 °C. According to their results, CFRP composites showed failure mode II and carbon fiber oxidation above 350 °C.

Figure 6(c) displays the ε_{max} (maximum strain) values for each specimen. The ε_{max} values were 0.019 ± 0.02% for all samples except for C350, which had a value of 0.011%. Although there was a slight variation in the ε_{max} values among the samples, they all exhibited brittle fracture regardless of the temperatures. The significant decrease in ε_{max} for C350 can be attributed to the accelerated failure resulting from the concentration of local force on a specific part of the fiber. Brittle fracture of the FRP composites can cause cracks and lead to mechanical failures, even under low mechanical loads during operational service [47].

Figure 6(d) illustrates the Young's modulus (E) values of the samples, which were 53.2, 55.4, 55.5, 54.7, 55.2, 55.2, and 52.0 GPa, respectively. This trend indicates that the carbon fibers played a significant role in transferring forces during the tensile test. In conclusion, the degradation of the epoxy matrix and the absence of the epoxy matrix layer

greatly impair the uniform distribution of tensile force, thereby affecting the mechanical properties. Zhou et al. [45] reported that epoxy resin loses its ability to transfer load between fibers and matrix above 300 ºC. Consequently, the mechanical properties of the C350 sample were significantly degraded, with σmax and εmax values of 0.605 GPa and 0.011%, respectively.

4. CONCLUSIONS

The thermo-mechanical and microstructural properties of carbon fiber reinforced plastic (CFRP) plates under elevated temperatures (50–350 ºC) were investigated. X-ray diffraction results confirmed the presence of CFRP composites. The full width half maximum (FWHM) initially decreased up to 150 ºC due to hardening of the polymers. However, it increased again with higher temperatures due to degradation and softening of the resin matrix. Scanning electron microscope images showed minimal defects in the C000–C150 samples, while the C200–C300 samples exhibited surface defects such as delamination and debonding between the fiber and matrix. The C350 sample showed significant decomposition of the resin matrix above T_d. The thermal conductivity (κ) changes closely followed the FWHM changes, with κ values of 0.70 W/mK for C000 and 0.18 W/mK for C350, attributed to phonon scattering intensified by decreased crystallinity. Tensile strength (σ_{max}) substantially increased to 1.10, 1.15, and 1.21 GPa for C050, C100, and C150, respectively, compared to 1.04 GPa of C000. In contrast, σ_{max} decreased in the C200–C350 samples, particularly in C350, which decreased by 40% to 0.605 GPa. The Young's modulus (E) showed similar values of approximately 50 GPa, indicating the primary influence of carbon fibers on mechanical properties. However, matrix degradation should also be considered, as it significantly contributes to force distribution. This factor is equally important in the thermal transport mechanism, highlighting the role of the polymer matrix in the thermo-mechanical performance of CFRP composites at elevated temperatures.

Data Availability Statement

Data available on request from the authors.

ACKNOWLEDGEMENT

This study was supported by the National Research Foundation of Korea (NRF-2021R1A4A1031201) for Sungmo Choi. Also, this study was supported by by the Basic Study and Interdisciplinary R&D Foundation Fund of the University of Seoul (2023) for Sang-il Kim.

REFERENCES

1. J. Hult and F. G. Rammerstorfer, *Engineering Mechanics of Fibre Reinforced Polymers and Composite Structures*, pp.1-287, Springer, Vienna (1994).
2. B. -H. Kang, O. -N. Hur, S. -K. Hong, and S. -H. Park, *Korean J. Met. Mater.* **60**, 694 (2022).
3. P. Morgan, *Carbon Fibers and Their Composites*, CRC Press, pp.1-1200, Boca Raton (2005).
4. D. Ozkan, M. S. Gok, and A. C. Karaoglanli, *Engineering Design Applications III: Structures, Materials and Processes*, pp.235-253, Springer, Cham (2020).
5. J. Matsui, *Reinf. Plast.* **43**, 187 (1997).
6. J. Matsui, *Reinf. Plast.* **43**, 485 (1997).
7. R. Balamuralikrishnan, and C.A. Jeyasehar, *Open. Civ. Eng. J.* **3**, 102 (2009).
8. I. Grabovac, *Compos. Pt. A-Appl. Sci. Manuf.* **34**, 847 (2003).
9. F. Ahmad, J. W. Hong, H. S. Choi, and M. K. Park, *Compos. Struct.* **135**, 276 (2016).
10. G. Williams, R. Trask, and I. Bond, *Compos. Pt. A-Appl. Sci. Manuf.* **38**, 1525 (2007).
11. B. Täljsten and L. Elfgren, *Compos. Pt. B: Eng.* **31**, 87 (2000).
12. C. Aksoylu, S. Yazman, Y. O. Özkılıç, L. Gemi, and M. H. Arslan, *Compos. Struct.* **249**, 112561 (2020).
13. A. Borri, M. Corradi, and A. Grazini, *Compos. Pt. B: Eng.* **36**, 143 (2005).
14. Y. Liu, B. Zwingmann, and M. Schlaich, *Polymers* **7**, 2078 (2015).
15. U. Meier, *Proc. Inst. Mech. Eng. Part B-J. Eng. Manuf.* **201**, 73 (1987).
16. W. Jay Rohleder, Jr., B. Tang, T. A. DOE, N. F. Grace, and C. J. Burgess, *Transp Res Record* **2050**, 169 (2008).
17. G. H. Xie, J. Yin, R. Liu, B. chen, and D. S. Cai, *Compos. Pt. B: Eng.* **111**, 235 (2017).
18. P. Feng, L. P. Ye, and J. G. Teng, *J. Compos. Constr.* **11**, 110 (2007).

19. I. Olofin and R. Liu, *Int. J. Civ. Eng.* **2**, 1 (2015).
20. M. Motavalli, C. Czaderski, and K. Pfyl-Lang, *J. Compos. Constr.* **15**, 194 (2011).
21. A. M. Pawlak, T. Górny, Ł. Dopierała and P. Paczos, *Metals*, **12**, 1470 (2022).
22. Y. Wei and S. A. Hadigheh, *Constr. Build. Mater.* **348**, 128654 (2022).
23. A. Al-Khafaji, A. El-Zohairy, M. Mustafic and H. Salim, *Buildings*, **12**, 873 (2022).
24. H. Ashrafi, M. Bazli, E. P. Najafabadi, and A. Vatani Oskouei, *Constr. Build. Mater.* **157**, 1001 (2017).
25. U. Berardi and N. Dembsey, *Polymers* **7**, 2276 (2015).
26. A. Chatterjee, *J. Appl. Polym. Sci.* **114**, 1417 (2009).
27. Y. chen, Z. chen, S. Xiao, and H. Liu, *Thermochim. Acta* **476**, 39 (2008).
28. H. Hajiloo, M. F. Green, and J. Gales, *Constr. Build. Mater.* **162**, 142 (2018).
29. J. Zhou and J. P. Lucas, *Polymer* **40**, 5513 (1999).
30. S. V. Levchik and E. D. Weil, *Polym. Int.* **53**, 1901 (2004).
31. M. Jarrah, E. P. Najafabadi, M. H. Khaneghahi, and A. V. Oskouei, *Constr. Build. Mater.* **190**, 38 (2018).
32. S. Cao, W. U. Zhis, and X. Wang, *J. Compos. Mater.* **43**, 315 (2009).
33. R. A. Hawileh, A. Abu-Obeidah, J. A. Abdalla, and A. Al-Tamimi, *Constr. Build. Mater.* **75**, 342 (2015).
34. L. Sorrentino, S. Turchetta, and C. Bellini, *Compos Struct* **168**, 549 (2019).
35. S. W. Lee, S. Han, S. Kim, and S. Choi, *J. Reinf. Plast. Compos*.**42**, 1220 (2023).
36. H. Wang, X. Zhang, and Y. Duan, *Inter. J. Adv. Manuf. Technol.* **96**, 2943 (2018).
37. J. M. Park, D. J. Kwon, Z. J. Wang, G. Gu, and K. L. DeVries, *Compos. Pt. A: Appl. Sci. Eng.* **47**, 156 (2013).
38. M. R. Wisnim, *Philos. Trans. R. Soc. A Math. Phys. Eng. Sci.* **370**, 1850 (2012).
39. S. Hasnmi, *Comprehensive Materials Processing, 1st ed.*, Elsevier, Dublin (2014).
40. S. Nunna, M. Maghe, R. Rana, E. J. Varley, J. Knorr Daniel B, J. M. Sands, C. Creighton, L. C. Henderson, and M. Naebe, *Materials* **12**, 1069 (2019).
41. D. M. Mustafa, S. Rostam, and S. B. Aziz, *Adv. Mater. Sci. Eng.* **2020**, 7914796 (2020).
42. A. Monshi, M. R. Foroughi, and M. R. Monshi, *World J. Nano Sci. Eng.* **2**, 154 (2012).
43. J. H. Robertson, *Acta Cryst. A* **35**, 350 (1979).
44. X. Liu, H. Luan, Y. Jinglin, S. Wang, S. Wang, and L. Copeland, *Carbohydr. Polym.* **242**, 116405 (2020).
45. H. Fujishiro, M. Ikebe, T. Kashima, and A. Amanaka, *Jap. J. Appl. Phys.* **36**, 5633 (1997).
46. E. Senis, I. O. Golosnoy, O. Thomsen, J. Barton, and S. Madsen, *21st International Conference on Composite Materials,* Xi'an ,China (2017).
47. R. Rolfes and U. Hammerschmidt, *Compos Sci and Tech* **54**, 45 (1995).
48. A. Zhou, Q. Qiu, C. L. Chow, and D. Lau, *Compos. Pt. A: Appl. Sci. Manuf.* **131**, 105802 (2020).
49. M. Kuhl, *IEEE Trans. Dielectr. Electr. Insul.* **8**, 182 (2001).
50. K. Wang, B. Young, and S. T. Smith, *Eng. Struct.* **33**, 2154 (2011).